

**Compression behavior of  $M_2\text{AlC}$  ( $M=\text{Ti, V, Cr, Nb, and Ta}$ ) phases to above 50 GPa**

Bouchaib Manoun\*

*Center for Study of Matter at Extreme Conditions (CeSMEC), Florida International University, VH-140,  
University Park, Miami, Florida 33199, USA**and Laboratoire d'Analyses, d'Essais et d'Environnement (L.A.E.E.), Département de Chimie, Faculté des Sciences "Dhar Mehraz,"  
Université Sidi Mohamed Ben Abdellah, 30000 Fès, Morocco*

R. P. Gulve and S. K. Saxena

*Center for Study of Matter at Extreme Conditions (CeSMEC), Florida International University, VH-140,  
University Park, Miami, Florida 33199, USA*

S. Gupta and M. W. Barsoum

*Department of Materials Science and Engineering, Drexel University, Philadelphia, Pennsylvania 19104, USA*

C. S. Zha

*Cornell High Energy Synchrotron Source (CHESS), Wilson Laboratory, Cornell University, Ithaca, New York 14853, USA*

(Received 6 April 2005; revised manuscript received 12 September 2005; published 20 January 2006)

The compression behavior of the hexagonal  $MAX$  phases  $M_2\text{AlC}$  ( $M=\text{Ti, V, Cr, Nb, and Ta}$ )—selected because they represent two series; a horizontal series in which the atomic number of the  $M$  element increases from 23 to 25 and a vertical series where the  $M$  element (V, Nb, or Ta) belongs to the VA group—were measured as a function of quasihydrostatic pressure up to 55 GPa, using a synchrotron radiation source and a diamond-anvil cell. No phase transformations were observed in any of these compounds. The contractions for the Ti- and V-containing compositions were higher along the  $c$  axis than along the  $a$  axis; the opposite was true for  $\text{Cr}_2\text{AlC}$  and  $\text{Nb}_2\text{AlC}$ . In  $\text{Ta}_2\text{AlC}$ , the shrinkages in both directions are almost identical. For  $\text{V}_2\text{AlC}$  the bulk modulus  $K_0$  is  $201 \pm 3$  GPa. As V is substituted by Nb,  $K_0$  increases by 4%. The  $K_0$  of  $\text{Ta}_2\text{AlC}$ , 251 GPa, is the highest reported for any  $MAX$  phase to date. For  $\text{Ti}_2\text{AlC}$ ,  $K_0$  is  $186 \pm 2$  GPa. As Ti is substituted by V,  $K_0$  increases by 8%. Surprisingly, the substitution of Ti or V by Cr leads to a reduction in  $K_0$  to  $165 \pm 2$  GPa. With the notable exception of  $\text{Cr}_2\text{AlC}$ , the agreement between experimental and calculated  $K_0$  values is acceptable. The presence of C in these structures appears to have a stabilizing effect on the  $M$ -Al bonds, presumably by attracting electrons to the  $M$ -X bonds.

DOI: [10.1103/PhysRevB.73.024110](https://doi.org/10.1103/PhysRevB.73.024110)

PACS number(s): 62.50.+p

**I. INTRODUCTION**

The  $M_{n+1}AX_n$  ( $MAX$ ) compounds, where  $n=1, 2,$  or  $3$ ,  $M$  is an early transition metal,  $A$  is an A-group (mostly IIIA and IVA) element, and  $X$  is C or N, have been studied extensively these last few years.<sup>1-5</sup> Based on the value of  $n$ , this class of materials form three groups, viz.  $M_2AX$  or 211,  $M_3AX_2$  or 312, and  $M_4AX_3$  or 413. The crystal structures of most of these phases—they number over 50—were first deciphered by Nowotny and co-workers in the 1960's.<sup>6</sup> These carbides adopt a hexagonal crystal structure consisting of layers of edge sharing  $MC_6$  octahedra and square-planar  $A$  layers. The edge sharing  $TiC_6$  octahedra are identical to those found in the rocksalt structure of the corresponding binary carbides  $MX$ .<sup>6</sup>

More recently the  $MAX$  phases have been shown to combine an unusual set of properties. They are good thermal and electrical conductors, relatively soft (Vickers hardness  $\approx 2-5$  GPa) and most readily machinable.<sup>1-5</sup> They are also exceedingly damage and thermal shock resistant. Some of them are elastically quite stiff with densities comparable to Ti metal and Debye temperatures  $>700$  K.<sup>7-9</sup> This combination of properties derives partially from the metallic nature of the bonding, partially from the layered nature of the structure

and partially from the fact that basal plane dislocations are mobile at all temperatures.

Recently Manoun *et al.*<sup>10-12</sup> reported on the compression behavior of  $\text{Ti}_3\text{Si}_{0.5}\text{Ge}_{0.5}\text{C}_2$ ,<sup>12</sup>  $\text{Zr}_2\text{InC}$ ,<sup>10</sup> and  $\text{Ti}_4\text{AlN}_3$ .<sup>11</sup> In all cases, no phase transitions were observed up to pressures of the order of 55 GPa. The isothermal bulk moduli  $K_0$  of these compounds, while high—216 GPa for  $\text{Ti}_4\text{AlN}_3$ , 183 GPa for  $\text{Ti}_3\text{Si}_{0.5}\text{Ge}_{0.5}\text{C}_2$ , and 127 GPa for  $\text{Zr}_2\text{InC}$ —were lower than those of near-stoichiometric TiN, TiC, and ZrC (300, 220, and 195 GPa, respectively) binaries.<sup>13</sup> In all cases, the relative shrinkage along the  $c$  direction with pressure was more severe than along the  $a$  direction. Similar results were obtained for  $\text{Ti}_3\text{SiC}_2$ .<sup>14</sup>

The bulk modulus of  $\text{Nb}_2\text{AsC}$ ,  $224 \pm 2$  GPa, measured recently,<sup>15</sup> is currently the highest for a  $MAX$  phase. In contradistinction to all other  $MAX$  phases reported to date, in  $\text{Nb}_2\text{AsC}$ , the contraction with pressure along the  $a$  direction is higher than along the  $c$  direction; in other words, the  $c/a$  ratio increases with applied pressure.

Sun *et al.*<sup>16,17</sup> carried out *ab initio* total energy calculations using the projector augmented wave method on  $M_2\text{AlC}$  ( $M=\text{Ti, V, Cr, Ta, and Nb}$ ). The  $K_0$  values—calculated from theory (see Table III)—were predicted to increase by 19 and 36 %, respectively, as Ti was substituted by V or Cr. They

also predicted that, as V is substituted by Nb or Ta,  $K_0$  would increase by 5 and 13 %, respectively.

The combination of easy machinability, relative low densities (in some of the phases) and high elastic constants, together with the possibility of extremely high damping<sup>18,19</sup> is one that to date had not been possible. Thus one motivation for this work was to identify compositions of potential technological interest. The second motivation was to directly measure the bulk moduli of these solids, and compare our experimental results with the theoretical work. As noted above, we chose to measure the bulk moduli of  $M_2\text{AlC}$  ( $M = \text{Ti, V, Cr, Nb, and Ta}$ ) phases. These compounds were selected because they represent two series; a horizontal series in which the atomic number of the  $M$  element increases from 23 to 25; and a vertical series where the  $M$  elements (V, Nb, and Ta) belong to the VA group. We were also interested in exploring the stability of these phases at high pressures.

## II. EXPERIMENTAL DETAILS

The processing details can be found elsewhere. In short, fully dense, predominantly single phase samples of  $\text{Ti}_2\text{AlC}$ ,<sup>20</sup>  $\text{V}_2\text{AlC}$ ,<sup>21</sup> and  $\text{Nb}_2\text{AlC}$ ,<sup>22</sup> were prepared by reactively hot isostatic pressing (HIP) the appropriate stoichiometric mixtures of powders of the constituent elements and/or appropriate carbides.

To fabricate the  $\text{Ta}_2\text{AlC}$  samples Ta, C, and Al powders (99% pure, -325 mesh, Alfa Aesar, Ward Hill, MA) were mixed in stoichiometric proportions, ball milled, cold pressed and placed in a graphite die in a vacuum hot press. The latter was evacuated and heated to 650 °C for 6 h, and then to 1600 °C. The sample was held at the maximum applied uniaxial pressure ( $\approx 30$  MPa) and temperature for 8 h. The  $\text{Cr}_2\text{AlC}$  samples were fabricated by reactive HIPing of Cr, Al, and graphite powders (99.9% and -325 mesh, Alfa Aesar, Ward Hill, MA). The powders were mixed in stoichiometric proportions and ball milled in a plastic container with alumina balls for 1 h. The mixed powders were sealed in borosilicate glass tubes, under mechanical vacuum and

heated to 650 °C for 10 h. This procedure led to the collapse of the glass tubes and allowed the powders to prereact. The collapsed tubes were placed in the HIP, heated at 10 °C/min to 650 °C, followed by a rate of 2 °C/min to 750 °C. The chamber was then pressurized with Ar gas to 70 MPa. Once pressurized, the heating resumed at 10 °C/min to 1200 °C, held at temperature for 12 h and furnace cooled. The pressure at 1200 °C was  $\approx 100$  MPa.

An online image plate recorded the angle-dispersive diffraction patterns of  $\text{V}_2\text{AlC}$  and  $\text{Ti}_2\text{AlC}$ ; the measurements were conducted at room temperature using synchrotron radiation at the High Pressure Collaborating Access Team (HP-CAT) beam line at the Advanced Photon Source (Chicago). A monochromatic beam—with a wavelength  $\lambda = 0.4066$  Å for  $\text{V}_2\text{AlC}$  and  $\lambda = 0.3678$  Å for  $\text{Ti}_2\text{AlC}$ —was focused to a 10  $\mu\text{m}$  spot size on the sample. For  $\text{Nb}_2\text{AlC}$  and  $\text{Ta}_2\text{AlC}$ , the x-ray diffraction patterns—using a  $\lambda = 0.496$  Å of a monochromatic beam focused down to a 35  $\mu\text{m}$  spot size—were collected at CHESS (Cornell University Ithaca, NY). Diffraction rings were recorded between  $2\theta = 1^\circ$  and  $35^\circ$ .

For  $\text{Cr}_2\text{AlC}$  the diffraction patterns were collected using energy dispersive mode at the bending magnet beamline of the Cornell High Energy Synchrotron Source (CHESS). A solid-state Ge detector, used to detect the diffracted energy, was calibrated with fluorescence standards of  $^{55}\text{Fe}$  and  $^{133}\text{Ba}$ , while the  $2\theta_0$  of  $11^\circ$  was attuned taking diffraction patterns of a gold standard.

Measurements were conducted at room temperature; powdered samples were pressurized using a gasketed diamond-anvil cell (DAC) with a 300 to 400  $\mu\text{m}$  culet. A 250  $\mu\text{m}$  initial thickness rhenium gasket, was indented to about 40–50  $\mu\text{m}$ . Since high purity Al does not undergo structural phase transition at high pressure, has low shear strength, as in our previous work,<sup>10–12,23,24</sup> it was the pressure-transmitting medium of choice. Also since its pressure-volume relation is well established<sup>25</sup> it also acted as a pressure marker. Powdered samples were placed between two pieces of Al foil ( $\approx 15$   $\mu\text{m}$  thickness) and packed in the 100–150  $\mu\text{m}$  hole.

TABLE I. Ambient pressure lattice parameters and unit cell volumes of  $M_2\text{AlC}$  compounds measured herein. Also listed are previous results. The space group adopted for all phases is  $P6_3/mmc$ .

$M_2\text{AlC}$	Ti	V	Cr	Nb	Ta
$a$ (Å)	$3.065 \pm 0.004$	$2.914 \pm 0.003$	$2.857 \pm 0.002$	$3.103 \pm 0.004$	$3.086 \pm 0.006$
	3.058 <sup>a</sup>	2.909 <sup>b</sup>	2.854 <sup>b</sup>	3.106 <sup>a</sup>	3.07 <sup>c</sup>
	3.052 <sup>b</sup>	2.925 <sup>d</sup>	2.848 <sup>d</sup>	3.107 <sup>c</sup>	3.099 <sup>f</sup>
	3.062 <sup>d</sup>			3.129 <sup>f</sup>	
$c$ (Å)	$13.71 \pm 0.03$	$13.19 \pm 0.03$	$12.81 \pm 0.02$	$13.93 \pm 0.03$	$13.85 \pm 0.04$
	13.624 <sup>a</sup>	13.127 <sup>b</sup>	12.82 <sup>b</sup>	13.888 <sup>a</sup>	13.8 <sup>c</sup>
	13.64 <sup>b</sup>	13.105 <sup>d</sup>	12.72 <sup>d</sup>	13.888 <sup>e</sup>	13.898 <sup>f</sup>
	13.673 <sup>d</sup>			13.895 <sup>f</sup>	
$V_0$ (Å) <sup>3</sup>	$111.6 \pm 0.6$	$97.0 \pm 0.7$	$90.6 \pm 0.5$	$116.2 \pm 0.7$	$114.4 \pm 0.7$

<sup>a</sup>Reference 28.

<sup>b</sup>Reference 29.

<sup>c</sup>Reference 6.

<sup>d</sup>Reference 16.

<sup>e</sup>Reference 22.

<sup>f</sup>Reference 30.

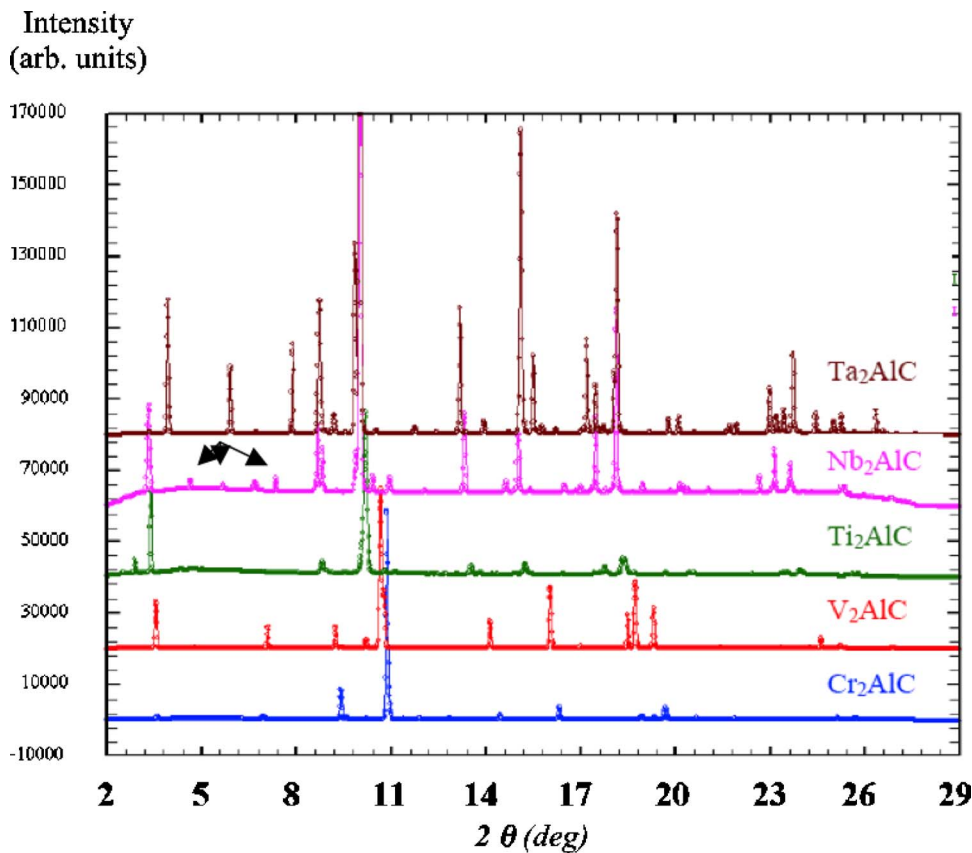


FIG. 1. (Color online) Ambient pressure x-ray powder diffraction patterns of  $M_2\text{AlC}$  phases studied in this work. Except for  $\text{Ta}_2\text{AlC}$ , all major peaks were assigned to the hexagonal structure ( $P6_3/mmc$ ). A few low intensity impurity peaks, which were not identified, were also observed in  $\text{Nb}_2\text{AlC}$  (arrows) and  $\text{Cr}_2\text{AlC}$  (the impurity peaks have very low intensity and can not be seen at this scale). The XRD spectrum of the  $\text{Ta}_2\text{AlC}$  sample, contained extra and overlapping peaks of another phase that we tentatively identified as a new  $\text{MAX}$  phase.

The FIT2D software<sup>26,27</sup> was employed to convert the image plate records into  $2\theta$ 's and intensities. All cell parameters were determined using least squares refinement on individually fitted peaks.

### III. RESULTS AND DISCUSSION

The x-ray powder diffraction patterns collected at 1 atm for  $\text{Cr}_2\text{AlC}$ ,  $\text{V}_2\text{AlC}$ ,  $\text{Ti}_2\text{AlC}$ ,  $\text{Nb}_2\text{AlC}$ , and  $\text{Ta}_2\text{AlC}$  are shown in Fig. 1. For all but  $\text{Ta}_2\text{AlC}$ , all major peaks were assigned to the hexagonal structure with the space group  $P6_3/mmc$ . A few low intensity impurity peaks, which were not identified, were also observed in  $\text{Nb}_2\text{AlC}$  and  $\text{Cr}_2\text{AlC}$ . Figure 2 shows typical high-pressure x-ray diffraction spectra for  $\text{Cr}_2\text{AlC}$ . Note that upon compression, most peaks remain visible until the highest pressure reached in this study.

In general the agreement between the unit cell parameters measured in this study, those previously reported,<sup>6,22,28–30</sup> and those predicted from the *ab initio* calculations<sup>16</sup> is acceptable (Table I). The XRD spectra of the  $\text{Ta}_2\text{AlC}$  sample, contained extra and overlapping peaks of another phase that we tentatively identified as a new  $\text{MAX}$  phase  $\text{Ta}_4\text{AlC}_3$ . The details of that study will be reported elsewhere.

Figure 3 plots the variations in lattice parameters versus applied quasihydrostatic pressure  $P$ . Second order polynomial least square fits resulted in the coefficients listed in Table II. From the results we note that (i) the contraction along the  $a$  direction with pressure is greater than along the  $c$  direction for  $\text{Nb}_2\text{AlC}$  and  $\text{Cr}_2\text{AlC}$ , (ii) the opposite is true for  $\text{Ti}_2\text{AlC}$  and  $\text{V}_2\text{AlC}$ , and (iii)  $\text{Ta}_2\text{AlC}$  is unique in that the

variations along the two orthogonal directions are almost identical.

Figure 4 plots the axial ratios  $(c/c_0)/(a/a_0)$  as a function of pressure. From this figure it is clear that for  $\text{Ti}_2\text{AlC}$  and

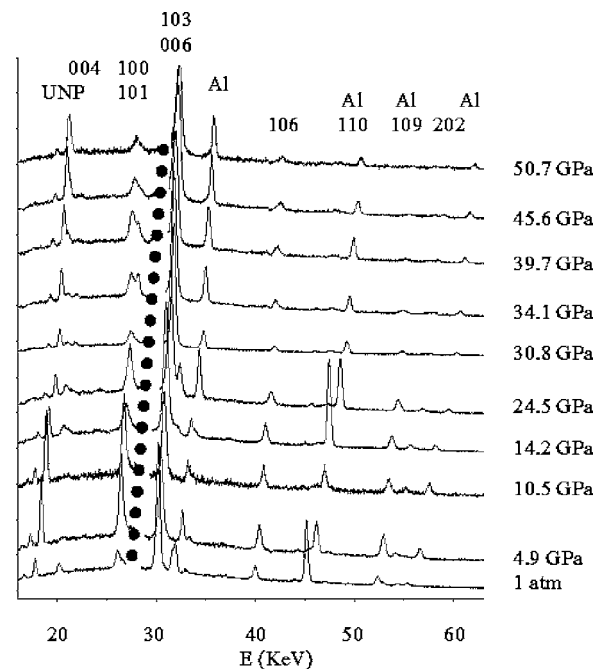


FIG. 2. X-ray diffraction patterns of  $\text{Cr}_2\text{AlC}$   $\text{MAX}$  phase to pressures up to 50.7 GPa. The 111 aluminum peak was removed for clarity. “UNP” stands for unidentified peak.

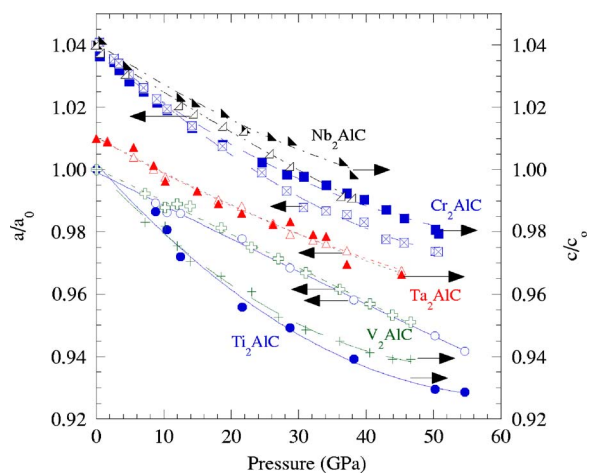


FIG. 3. (Color online) Pressure dependencies of the  $a/a_0$  (left axis) and  $c/c_0$  (right axis) for  $M_2\text{AlC}$  phases studied in this work. Curves are separated vertically for clarity; the symbol colors and those of the letters representing the various compounds are matched. The contraction along the  $a$  direction with pressure is greater than along the  $c$  direction for  $\text{Nb}_2\text{AlC}$  and  $\text{Cr}_2\text{AlC}$ ; the opposite is true for  $\text{Ti}_2\text{AlC}$  and  $\text{V}_2\text{AlC}$ ;  $\text{Ta}_2\text{AlC}$  is unique in that the variations along the two orthogonal directions are almost identical. Note the lines are least square fits of the data points.

$\text{V}_2\text{AlC}$  the axial ratio decreases before increasing slightly at pressures above  $\approx 30$  GPa. For  $\text{Cr}_2\text{AlC}$  and  $\text{Nb}_2\text{AlC}$ , the axial ratio increases with pressure, before leveling out at higher pressures. For  $\text{Ta}_2\text{AlC}$ , the axial ratio hovers around unity before decreasing slightly.

From relative unit cell volume versus pressure plots (Fig. 5) it is clear that  $\text{Cr}_2\text{AlC}$  possesses the lowest bulk modulus,  $\text{Ta}_2\text{AlC}$  the highest, with those of  $\text{V}_2\text{AlC}$ ,  $\text{Nb}_2\text{AlC}$ , and  $\text{Ti}_2\text{AlC}$  in between. Least squares fit of these data yield the results listed in Table III. Fitting the same results to the Birch-Murnaghan equation<sup>31</sup>

$$P = 3/2K_0[(V/V_0)^{-7/3} - (V/V_0)^{-5/3}] \\ \times \{1 + 3/4(K_0' - 4)[(V/V_0)^{-2/3} - 1]\}$$

yields  $K_0$  values that vary from a low of  $165 \pm 2$  GPa for  $\text{Cr}_2\text{AlC}$ , to a high of  $251 \pm 3$  GPa for  $\text{Ta}_2\text{AlC}$ , with the others in between (Table III). The calculated pressure derivative values  $K_0'$  are also listed in Table III. For  $\text{V}_2\text{AlC}$ ,  $K_0$  is  $201 \pm 3$  GPa. As V is substituted by Nb,  $K_0$  increases by 4%; for  $\text{Ti}_2\text{AlC}$ ,  $K_0$  is  $186 \pm 2$  GPa. As Ti is substituted by V,  $K_0$

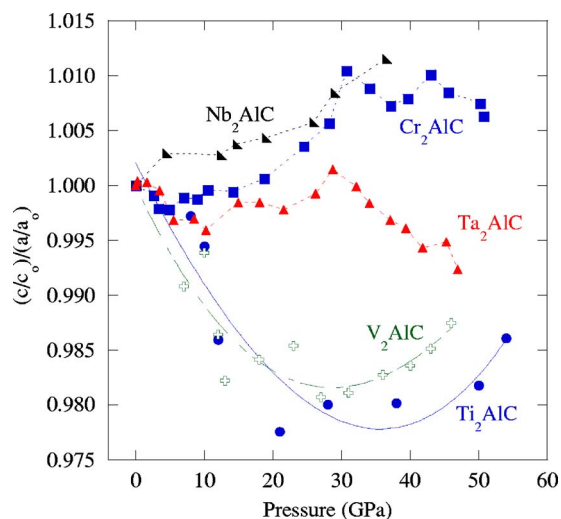


FIG. 4. (Color online) Axial ratio  $(c/c_0)/(a/a_0)$  versus pressure  $P$ . For  $\text{Ti}_2\text{AlC}$  and  $\text{V}_2\text{AlC}$  the ratio decreases before increasing slightly. For  $\text{Cr}_2\text{AlC}$  and  $\text{Nb}_2\text{AlC}$  the ratio increases. For  $\text{Ta}_2\text{AlC}$ , the axial ratio fluctuates around 1 before decreasing slightly.

increases by 8%. Surprisingly, the substitution of Ti by Cr leads to reduction in  $K_0$  to  $165 \pm 2$  GPa.

Based on this work it is clear that the nature of the  $M$  element has a large effect on the bulk moduli of the  $\text{MAX}$  phases. In a recent paper, Music *et al.*,<sup>32</sup> using *ab initio* calculations, showed that, in  $\text{Sc}_2\text{AlC}$  with  $A = \text{Al, Ga, In, and Tl}$ , the bulk modulus was not affected much by the  $A$  substitution. This is also true in  $\text{Ti}_3\text{AlC}_2$  phases ( $A = \text{Si, Ge, Al}$ ) where the  $A$  element did not have much effect on the bulk modulus, which varied from 206 for  $\text{Ti}_3\text{SiC}_2$  (Ref. 14) to 226 for  $\text{Ti}_3\text{AlC}_2$ .<sup>33</sup>

The  $K_0$  values reported herein are in line with previous  $\text{MAX}$  phase results in that these solids are elastically quite stiff.<sup>10–12,14,15</sup> At this time,  $\text{Ta}_2\text{AlC}$  has the highest bulk modulus of any  $\text{MAX}$  phase. Also in line with previous work is the stability of these phases under quasi-hydrostatic pressure. To date all  $\text{MAX}$  phases have been stable up to  $\approx 50$  GPa.

The results obtained in this work are useful in shedding important light on the bonding in these phases. As noted above, the only  $\text{MAX}$  phase to date for which the pressure contraction along the  $a$  direction was greater than the  $c$  direction was  $\text{Nb}_2\text{AlC}$ .<sup>15</sup> However, since  $\text{Nb}_2\text{AlC}$  and  $\text{Cr}_2\text{AlC}$  (Fig. 3, Table II) behave in the same way, this is no longer the case. From a bonding point of view, this result implies

TABLE II. Relative lattice parameter changes with pressure  $P$ .  $P_0$  defines the units used and is equal to 1 GPa. The correlation coefficient values in all cases were greater than 0.99.

$M_2\text{AlC}$	Pressure range	$a/a_0 = 1 + \beta P/P_0 + \gamma (P/P_0)^2$	$c/c_0 = 1 + \beta P/P_0 + \gamma (P/P_0)^2$
Ti	1 atm–55 GPa	$1 - 0.0011P/P_0 + 7 \times 10^{-7}(P/P_0)^2$	$1 - 0.0024P/P_0 + 2 \times 10^{-5}(P/P_0)^2$
Cr	1 atm–51 GPa	$1 - 0.0021P/P_0 + 2 \times 10^{-5}(P/P_0)^2$	$1 - 0.0017P/P_0 + 1 \times 10^{-5}(P/P_0)^2$
V	1 atm–47 GPa	$1 - 0.0010P/P_0 - 7 \times 10^{-7}(P/P_0)^2$	$1 - 0.0022P/P_0 + 2 \times 10^{-5}(P/P_0)^2$
Nb	1 atm–38 GPa	$1 - 0.0014P/P_0 + 3 \times 10^{-6}(P/P_0)^2$	$1 - 0.0014P/P_0 + 9 \times 10^{-6}(P/P_0)^2$
Ta	1 atm–47 GPa	$1 - 0.0012P/P_0 + 6 \times 10^{-6}(P/P_0)^2$	$1 - 0.0012P/P_0 + 5 \times 10^{-6}(P/P_0)^2$

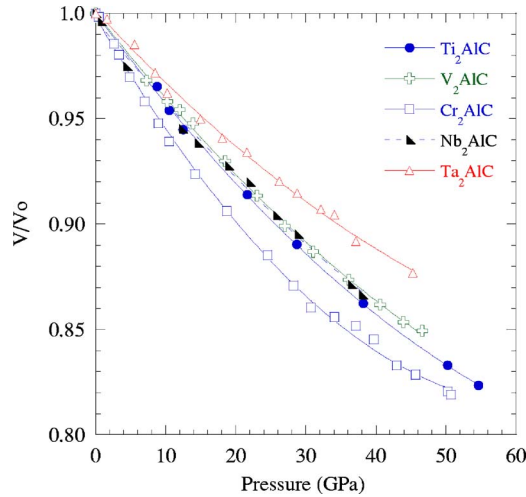


FIG. 5. (Color online) Relative volume of  $M_2\text{AlC}$  phases studied in this work as a function of pressure. Clearly,  $\text{Cr}_2\text{AlC}$  possesses the lowest bulk modulus,  $\text{Ta}_2\text{AlC}$  the highest, with those of  $\text{V}_2\text{AlC}$ ,  $\text{Nb}_2\text{AlC}$ , and  $\text{Ti}_2\text{AlC}$  in between. Lines shown are least square fits of the data points.

that contraction of the  $M$ - $X$  bonds (along the  $a$  direction) is higher than along the  $M$ -Al bonds. In other words, the latter are more resistant to deformation than the former. Based on these results it appears that the Nb-Al bonds are stronger than the Nb-C bonds. This is a noteworthy result because—based on the melting points of the early transition metal binary carbides—the  $M$ -C bonds are believed to be some of the strongest known. For example, the melting point of NbC is 3600 °C. Those of  $\text{Nb}_2\text{Al}$  and  $\text{Nb}_3\text{Al}$  on the other hand, are  $\approx 2000$  °C. Similar arguments can be made concerning the Ta-Al bonds in comparison to the Ta-C bonds. According to Fig. 3, they must be quite comparable; again a somewhat surprising conclusion given that the melting point of TaC is 3985 °C, while that of  $\text{Ta}_2\text{Al}$  is  $\approx 2100$  °C. Note that since the  $\text{MAX}$  phases are near closed packed, the arguments about relative bond strengths and their relationships to melting points, are more tenable than in more open or complex structures.

It thus appears that the presence of C in the interstitial sites of the  $M$  octahedra has a stabilizing effect on the  $M$ -Al bonds. One explanation is that the  $X$  atoms attract electrons, that would otherwise go into antibonding  $M$ -Al orbitals. This not only would explain the stability of the  $M$ -Al

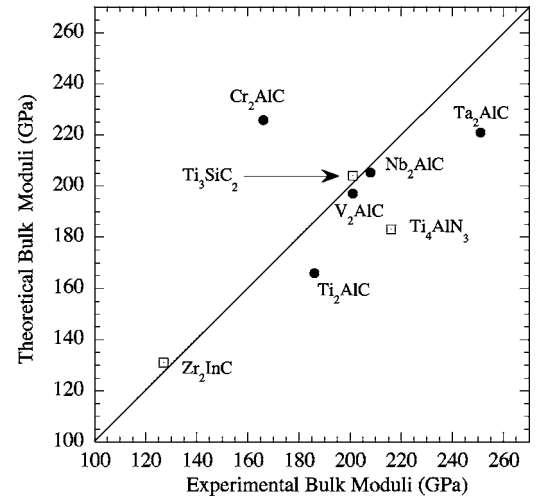


FIG. 6. Theoretical versus experimental bulk moduli. The agreement between our results and those deduced from recent *ab initio* calculations is mixed. Also included are previous results for other  $\text{MAX}$  phases (Refs. 10, 11, 14, and 34). For  $\text{V}_2\text{AlC}$  and  $\text{Nb}_2\text{AlC}$  the agreement is excellent; for  $\text{Ti}_2\text{AlC}$  it is within 10%. The *ab initio* calculations (Ref. 17) underestimate the bulk modulus of  $\text{Ta}_2\text{AlC}$  by  $\approx 15\%$ , and overestimate the bulk modulus of  $\text{Cr}_2\text{AlC}$  by almost 40%. The symbols are data generated in this paper; the square symbols are those for  $\text{Zr}_2\text{InC}$  (Ref. 10),  $\text{Ti}_3\text{SiC}_2$  (Ref. 14), and  $\text{Ti}_4\text{AlN}_3$  (Refs. 11 and 34).

bonds in the ternaries, but also their relative weakness in the binary  $M$  aluminides. This conclusion is bolstered by recent *ab initio* calculations that have shown that in the  $M_2\text{AlC}$  phases of the first transition metal series, as well as  $\text{Nb}_2\text{AlC}$ , the C atoms always carry a negative charge.<sup>28</sup> Along the same lines Music *et al.*,<sup>32</sup> using *ab initio* calculations, showed that the antibonding states in the vicinity of the Fermi level for  $\text{Sc}_2\text{AlC}$  (where  $A=\text{Al, Ga, In, and Tl}$ ), result in a weakening of the overall bonding. These comments notwithstanding, it is hereby acknowledged that more work is needed to explore the validity of some of these arguments.

The results also show that  $K_0$  increases as Nb replaces V and Ta replaces Nb. The agreement between our results and those deduced from recent *ab initio* calculations (Fig. 6) is mixed. (For completeness, Fig. 6 includes previous results for other  $\text{MAX}$  phases.<sup>10,11,14,34</sup>) For  $\text{V}_2\text{AlC}$  and  $\text{Nb}_2\text{AlC}$  the agreement is excellent; for  $\text{Ti}_2\text{AlC}$  it is within 10%. The *ab initio* calculations, however, underestimate the bulk modulus

TABLE III. Relative unit cell volume changes with pressure and summary of experimental and calculated bulk moduli. The pressure derivatives  $K_0'$  are also given. All correlation coefficient values were  $>0.995$ . Also included are *ab initio* total energy calculation results by Sun *et al.* (Ref. 17).

$M_2\text{AlC}$	$V/V_0 = \alpha + \beta P/P_0 + \gamma (P/P_0)^2$	$K_0$ (GPa)	$K_0'$	$K_0$ (GPa) Ref. 17
Ti	$1 - 0.0045P/P_0 + 2 \times 10^{-5}(P/P_0)^2$	$186 \pm 2$	$4.0 \pm 0.1$	166
V	$1 - 0.0043P/P_0 + 2 \times 10^{-5}(P/P_0)^2$	$201 \pm 3$	$4.05 \pm 0.13$	195
Cr	$1 - 0.0058P/P_0 + 4 \times 10^{-5}(P/P_0)^2$	$165 \pm 2$	$4.1 \pm 0.1$	226
Nb	$1 - 0.0041P/P_0 + 2 \times 10^{-5}(P/P_0)^2$	$209 \pm 2$	$3.95 \pm 0.15$	205
Ta	$1 - 0.0036P/P_0 + 2 \times 10^{-5}(P/P_0)^2$	$251 \pm 3$	$4.5 \pm 0.2$	221

of Ta<sub>2</sub>AlC by  $\approx 14\%$ , while overestimating the bulk modulus of Cr<sub>2</sub>AlC by  $\approx 37\%$ . The latter is the most surprising result of this work. However, in line with the aforementioned discussion, it is possible that Cr<sub>2</sub>AlC has too many electrons that are forced into antibonding orbitals. The anomalous behavior of Cr<sub>2</sub>AlC is confirmed by its relatively low—1450 °C—peritectic decomposition temperature and a relatively high thermal expansion coefficient ( $\approx 12 \times 10^{-6} \text{ }^\circ\text{C}^{-1}$ ).<sup>35</sup> This structural destabilization is also clearly seen in a 7% drop in the energy of the highest-energy Raman vibrational mode—involving the motion of the *A* and *M* atoms along the *c* axis—of Cr<sub>2</sub>AlC relative to the Ti and V containing structures.<sup>36</sup>

Lastly we note that at  $\approx 14$  GPa, a shoulder—centered at  $\approx 1.207 \text{ \AA}$ —to the left of the (116) diffraction peak of V<sub>2</sub>AlC appeared. With increasing pressure the intensity of the peak increases, up to 36.1 GPa when it starts decreasing again. The reason for the extra peak and its behavior is unclear at this time. However, at  $\approx 18.5$  GPa the Al peak intensity was found to decrease dramatically, probably as a result of one of the Al disks leaking out and therefore the sample may start bridging the anvil. Whether the two events are correlated is, again, unclear and more work is required to understand this response.

#### IV. CONCLUSIONS

Using a synchrotron radiation source and a diamond-anvil cell, we measured the pressure dependencies of the lattice parameters of selected *M*<sub>2</sub>AlC phases. Up to a pressure of 55 GPa, no phase transformations were observed. The contractions in Ti<sub>2</sub>AlC and V<sub>2</sub>AlC compounds were higher

along the *c* than along the *a* axes; the opposite was true for Cr<sub>2</sub>AlC and Nb<sub>2</sub>AlC. For Ta<sub>2</sub>AlC, the shrinkages in both directions were almost identical. Going down the VA group results in a systematic increase in *K*<sub>0</sub>. The *K*<sub>0</sub> of Ta<sub>2</sub>AlC of 251 GPa, is the highest reported for any MAX phase to date. Going across the row of *M* elements, the bulk modulus increases before decreasing. This reduction in modulus of Cr<sub>2</sub>AlC relative to V<sub>2</sub>AlC, was not predicted, and is possibly a reflection of the fact that Cr<sub>2</sub>AlC may have too many electrons, that, in turn are pushed into antibonding orbitals. Furthermore, the presence of C in the structure has a stabilizing effect on the *M*-Al bonds, presumably by pulling electrons away from those bonds into the *M*-*X* bonds.

#### ACKNOWLEDGMENTS

This work was partially supported by an ONR (Grant No. N00421-03-C-0085) to Drexel U. This work was also financially supported by a grant from the National Science Foundation (Grant No. DMR 0231291). Bouchaib Manoun would like to thank El Bali and Lachkar for their support, this work is a part of his second Doctorate which he will defend in L.A.E.E. Laboratory at the Department of Chemistry, Faculty of Sciences “Dhar Mehraz,” Université Sidi Mohamed Ben Abdellah, 30000 Fès, Morocco. Part of the work was conducted at Cornell High Energy Synchrotron Source (CHESS), supported by a NSF grant and NIH/NIGMS under Grant No. DMR 0225180. HPCAT is a collaboration among the Carnegie Institution, Lawrence Livermore National Laboratory, the University of Hawaii, the University of Nevada Las Vegas, and the Carnegie/DOE Alliance Center (CDAC). We thank the HPCAT staff especially M. Somayazulu for technical assistance.

\*Author to whom correspondence should be addressed. Electronic address: manounb@fiu.edu

<sup>1</sup>M. W. Barsoum, Prog. Solid State Chem. **28**, 201 (2000).

<sup>2</sup>M. W. Barsoum and T. El-Raghy, Am. Sci. **89**, 336 (2000).

<sup>3</sup>M. W. Barsoum and T. El-Raghy, J. Am. Ceram. Soc. **79**, 1953 (1996).

<sup>4</sup>M. W. Barsoum and T. El-Raghy, Metall. Mater. Trans. A **30**, 363 (1999).

<sup>5</sup>M. W. Barsoum and M. Radovic, in *Encyclopedia of Materials: Science and Technology*, edited by R. W. C. K. H. J. Buschow, M. C. Flemings, E. J. Kramer, S. Mahajan, and P. Veysiere (Elsevier, Amsterdam, 2004).

<sup>6</sup>H. Nowotny, Prog. Solid State Chem. **2**, 27 (1970).

<sup>7</sup>P. Finkel, M. W. Barsoum, and T. El-Raghy, J. Appl. Phys. **87**, 1701 (2000).

<sup>8</sup>P. Finkel *et al.*, Phys. Rev. B **70**, 085104 (2004).

<sup>9</sup>S. E. Lofland, J. D. Hettinger, K. Harrell, P. Finkel, S. Gupta, M. W. Barsoum, and G. Hug, Appl. Phys. Lett. **84**, 508 (2004).

<sup>10</sup>B. Manoun, S. K. Saxena, H. P. Liermann, R. P. Gulve, E. Hoffman, M. W. Barsoum, G. Hug, and C. S. Zha, Appl. Phys. Lett. **85**, 1514 (2004).

<sup>11</sup>B. Manoun, S. K. Saxena, and M. W. Barsoum, Appl. Phys. Lett. **86**, 101906 (2005).

<sup>12</sup>B. Manoun, H. P. Liermann, R. P. Gulve, S. K. Saxena, A. Ganguly, M. W. Barsoum, and C. S. Zha, Appl. Phys. Lett. **84**, 2799 (2004).

<sup>13</sup>H. O. Pierson, *Handbook of Refractory Carbides and Nitrides* (Noyes Publications, Westwood, NJ, 1996).

<sup>14</sup>A. Onodera, H. Hirano, T. Yuasa, N. F. Gao, and Y. Miyamoto, Appl. Phys. Lett. **74**, 3782 (1999).

<sup>15</sup>R. S. Kumar, S. Rekhi, A. L. Cornelius, and M. W. Barsoum, Appl. Phys. Lett. **86**, 111904 (2005).

<sup>16</sup>Z. Sun, R. Ahuja, S. Li, and J. M. Schneider, Appl. Phys. Lett. **83**, 899 (2003).

<sup>17</sup>Z. Sun *et al.*, Solid State Commun. **129**, 589 (2004).

<sup>18</sup>M. W. Barsoum, M. Radovic, T. Zhen, P. Finkel, and S. R. Kalidindi, Phys. Rev. Lett. **94**, 085501 (2005).

<sup>19</sup>M. W. Barsoum *et al.*, Nat. Mater. **2**, 107 (2003).

<sup>20</sup>M. W. Barsoum, M. Ali, and T. El-Raghy, Metall. Mater. Trans. A **31**, 1857 (2000).

<sup>21</sup>S. Gupta and M. W. Barsoum, J. Electrochem. Soc. **151**, D24 (2004).

<sup>22</sup>I. Salama, T. El-Raghy, and M. W. Barsoum, J. Alloys Compd. **347**, 271 (2002).

<sup>23</sup>H. P. Liermann, A. K. Singh, B. Manoun, S. K. Saxena, V. B. Prakupenka, and G. Shen, Int. J. Refract. Met. Hard Mater. **22**,

- 129 (2004).
- <sup>24</sup>H. P. Liermann, A. K. Singh, B. Manoun, S. K. Saxena, and C. S. Zha, *Int. J. Refract. Met. Hard Mater.* **23**, 109 (2005).
- <sup>25</sup>R. G. Greene, H. Luo, and A. L. Ruoff, *Phys. Rev. Lett.* **73**, 2075 (1994).
- <sup>26</sup>A. P. Hammersley (unpublished).
- <sup>27</sup>A. P. Hammersley, S. O. Svensson, M. Hanfland, A. N. Fitch, and D. Häusermann, *High Press. Res.* **14**, 235 (1996).
- <sup>28</sup>G. Hug, M. Jaouen, and M. W. Barsoum, *Phys. Rev. B* **71**, 024105 (2005).
- <sup>29</sup>J. Schuster, H. Nowotny, and C. Vaccaro, *J. Solid State Chem.* **32**, 213 (1980).
- <sup>30</sup>R. Ahuja (private communication).
- <sup>31</sup>F. Birch, *J. Geophys. Res.* **83**, 1257 (1978).
- <sup>32</sup>D. Music, Z. Sun, and J. M. Schneider, *Solid State Commun.* **133**, 381 (2005).
- <sup>33</sup>B. Manoun (unpublished).
- <sup>34</sup>B. Holm, R. Ahuja, S. Li, and B. Johansson, *J. Appl. Phys.* **91**, 9874 (2002).
- <sup>35</sup>T. El-Raghy (private communication).
- <sup>36</sup>J. E. Spanier, S. Gupta, M. Amer, and M. W. Barsoum, *Phys. Rev. B* **71**, 012103 (2005).